

Roles of grain size and strain on antiferromagnetic order in nanocrystalline chromium

M. R. Fitzsimmons

Manuel Lujan, Jr. Neutron Scattering Center, Los Alamos National Laboratory, Los Alamos, New Mexico 87545

J. A. Eastman

Materials Science Division, Argonne National Laboratory, Argonne, Illinois 60439

R. B. Von Dreele

Manuel Lujan, Jr. Neutron Scattering Center, Los Alamos National Laboratory, Los Alamos, New Mexico 87545

L. J. Thompson

Materials Science Division, Argonne National Laboratory, Argonne, Illinois 60439

(Received 7 February 1994)

Neutron-diffraction investigations of powder and consolidated ultrafine-grain-sized chromium samples indicate that antiferromagnetic order in the body-centered-cubic phase of this material can be suppressed to well below the Néel temperature of coarse-grained and single-crystal chromium. The suppression is correlated strongly with decreasing grain size. Antiferromagnetic order was not observed in powder or in consolidated samples with grain sizes less than 16 nm, indicating that free surfaces and grain boundaries play the same role in preventing antiferromagnetic order with the structure of bulk chromium. Antiferromagnetic order was observed in nanocrystalline samples with grain sizes greater than 19 nm at 20 K. No correlation is seen between the Néel temperature and the degree of long-range microstrain, or with contents of light-element impurities in the samples. Even in cases where antiferromagnetic order is detected, the transversely polarized AF_1 spin-density-wave magnetic phase is never seen. While this may suggest that spin-density-wave phases do not occur in nanocrystalline chromium, the presence of the longitudinally polarized AF_2 spin-density-wave phase cannot be ruled out unambiguously.

I. INTRODUCTION

Interesting magnetic behavior has been observed in many nanophase materials. Data from small-angle neutron-scattering studies of consolidated nanocrystalline iron have been interpreted as indicating that magnetic domain sizes can be much larger than the grain size, but that grain boundary regions are only weakly magnetic compared to grain interiors.¹ The latter interpretation is in contradiction to conclusions drawn from some Mössbauer spectroscopy measurements, which suggest an enhancement of the magnetic hyperfine structure in nanocrystalline iron is due to an increase in the magnetization of the interfacial component.² In nickel, however, the magnetic hyperfine structure attributed to the interfacial component is reported to be somewhat diminished.²

A number of magnetic properties of materials are predicted to be grain size dependent. Fine particles are expected to exhibit single domain behavior below critical sizes ranging from 10 nm for low-anisotropy high-magnetization materials such as iron, to 1 μm for highly anisotropic low-magnetization hexagonally-structured oxides.³ Small particles may behave superparamagnetically at temperatures where their coarse-grained equivalents are ferromagnetic. For instance, iron and $\gamma\text{-Fe}_2\text{O}_3$ particles with sizes less than 20 and 50 nm, respectively, are expected to be superparamagnetic rather than ferromagnetic.³

Magnetic phase-transition temperatures have been observed to depend on grain or particle size. Large reductions of the Curie temperatures of iron⁴ and nickel⁵ have been reported for nanocrystalline materials. The saturation magnetization was also found to decrease compared to values in coarse-grained materials in some studies of nanocrystalline iron⁶ and nickel,⁵ while in another study of these same materials, no grain-size dependent behavior was observed.⁷

Recently, Fitzsimmons *et al.*⁸ reported the suppression of antiferromagnetic ordering to below 20 K in the body-centered-cubic (bcc) phase of a consolidated nanocrystalline chromium sample with an 11-nm-average grain size, since no magnetic Bragg reflection corresponding to the magnetically ordered bcc phase was observed. While the bcc phase was not antiferromagnetically ordered (at least above 20 K), a magnetic Bragg reflection attributed to the *A*-15 chromium phase (with the structure of Cr_3O) was observed at 20 K, but not at 150 or 300 K, suggesting that the *A*-15 phase became antiferromagnetically ordered at low temperatures. A detailed study of the relative importance of various microstructural features of the sample that were responsible for the suppression of antiferromagnetism in the bcc phase was beyond the scope of this earlier study, although it was noted that strain and impurities could be at least partially responsible for the change in behavior, since the magnetic properties of coarse-grained and single-crystal chromium

can be sensitive to these quantities.^{9,10}

Alternatively, the suppression of antiferromagnetism in bcc chromium may be due to the small grain size of the particles, which, if too small, may preclude the development of the spin-density wave that modulates antiferromagnetic ordering in bulk chromium.¹¹ The wavelengths of the two spin-density-wave structures found in single-crystal and coarse-grained polycrystalline chromium are believed to be on the order of 6 nm.¹² The smallest volume of material containing a single magnetic domain, i.e., the region in which the antiferromagnetic structure is correlated, in single-crystal chromium is reported to be approximately 3.2×10^{-16} cm³.¹³ This volume corresponds to a cube with dimension of about 68 nm. By reducing grain sizes below either the wavelength of the spin-density wave or the magnetic domain size, changes in the antiferromagnetic ordering of nanocrystalline chromium might be induced.

Motivation for this idea is found in the study of the transition element magnet $\text{Fe}_{73.5}\text{CuNb}_3\text{Si}_{13.5}\text{B}_9$.^{14,15} In this study, Herzer reported an improvement in soft magnetic properties of the material (its permeability increases) as grain size was reduced from 150 to 10 nm. This behavior is attributed to a suppression of the magnetocrystalline anisotropy in the grains that occurs when the structural correlation length of the small particles is comparable to or less than the ferromagnetic exchange length (about 35 nm for this material). While the magnetic properties of chromium are considerably different from those of $\text{Fe}_{73.5}\text{CuNb}_3\text{Si}_{13.5}\text{B}_9$, the relationship between the domain size or the wavelength of a spin-density-wave structure to the size of a chromium grain may be similarly important in determining magnetic properties of ultrafine-grained chromium.

Recently, Tsunoda, Nakano, and Matsuo¹⁶ reported that the antiferromagnetic structure of nanocrystalline bcc chromium powder was different from that of coarse-grained material based upon results from a neutron powder-diffraction study. By reducing the grain size of chromium powder, a commensurate antiferromagnetically ordered structure (called the AF_0 phase) was believed to be favored over the transversely (AF_1) and longitudinally (AF_2) polarized incommensurate spin-density-wave structures.¹⁶ They speculated that the limitation of translational symmetry imposed upon small particles disturbs the Fermi surface of chromium, from which chromium derives its magnetic properties, thus, making the spin-density wave unstable. Bacon and Cowlam⁹ previously reported that the AF_0 phase was stabilized to lower temperatures as the grain size of heavily crushed coarse-grained chromium powder was reduced to less than 0.1 μm . Neither of these studies reported any grain-size dependent change in the Néel temperature.

The present investigation was undertaken to determine what features of nanocrystalline chromium are most important in controlling the suppression of antiferromagnetism in the bcc phase. Systematic neutron-diffraction studies were made of the effects of grain size, consolidation, strain, and air exposure on the presence of antiferromagnetic order.

II. SAMPLE PREPARATION

Samples were prepared by vaporizing chromium chips (99.9994% pure) in an electron-beam-heated gas-condensation system.¹⁷ Powders consisting of agglomerated nanometer-scale individual grains were produced by collisions of chromium vapor with controlled pressures of gas in the chamber. Two separate preparation conditions were used. In the first, the oxygen pressure in the system was maintained as low as possible in an attempt to promote the formation of the A -15 chromium phase.^{18,19} The vacuum chamber was evacuated to approximately 5×10^{-5} Pa, and then backfilled with 27 Pa of 99.9999% pure helium. For the second preparation, oxygen was admitted to a pressure of 13 mPa after pumping the chamber to a pressure of 5×10^{-5} Pa, and then helium was added to bring the total pressure in the chamber again to 27 Pa. These conditions were expected to suppress the formation of the chromium A -15 phase and promote the formation of the normal bcc phase.^{18,19}

Nanocrystalline powders were collected on a liquid-nitrogen-cooled plate located in the chamber. After collection, some of the powders were transferred under vacuum conditions into quartz ampules that were then backfilled with approximately 0.5 atm. of helium and sealed to prevent exposure of the powder to air. The contents of the quartz ampules were later transferred into a helium-filled glove box and then sealed in vanadium cans. Vanadium cans were used as sample holders in the neutron-diffraction experiments. These procedures allowed neutron data to be acquired from material prepared under both preparation conditions without exposure to air.

III. NEUTRON-DIFFRACTION MEASUREMENTS

Neutron-diffraction data were obtained from four samples in the present investigation. Sample A consisted of powder (0.98 g) from the initial evaporation with no intentional oxygen or air exposure. Sample B (1.3 g) came from the same evaporation as sample A , but this powder was collected from the cold plate and chamber walls after opening the vacuum chamber to air. A second portion of this air-exposed powder was subsequently consolidated under a pressure of 1.4 GPa in vacuum to form a 0.3 g pellet of compacted nanocrystalline chromium, which was then transferred into a vanadium can in helium. This sample is referred to as sample C . Sample D consisted of powder (0.3 g) from the second evaporation, produced with 13 mPa of oxygen in the chamber. Like sample A , this powder had no air exposure. Comparisons were also made with neutron diffraction data from a compacted nanocrystalline sample and a coarse-grained control sample from our previous study of chromium.⁸ These two samples are referred to as samples E and F , respectively, in the present work.

Time-of-flight neutron-diffraction measurements were made using the high-intensity powder diffractometer (HIPD) at the Manuel Lujan Jr. Neutron Scattering Center.²⁰ Diffraction observations sampling d -spacings ranging from 0.35 to 4 Å were obtained from all four

samples at 20 K. Diffraction data were also obtained from sample *A* at higher temperatures of 51, 102, 152, and 300 K. A portion of the diffraction data from sample *A* taken at 20 K is shown in Fig. 1. Rietveld refinements of the neutron data, which included more than forty Bragg reflections with different d spacings, using the general structure analysis system (Refs. 21–23), determined the contents of secondary phases, as well as the average microstrain distributions, particle sizes, Debye-Waller parameters, and magnetic moments (when a magnetic reflection was observed) in the samples.

Samples *A* and *D* (the two samples with no prior air exposure) were found to contain only the bcc phase of chromium, with no sign of any secondary phases. This observation is surprising in light of the results of Kimoto and Nishida¹⁸ and Granqvist, Milanowski, and Buhrman,¹⁹ who found that nanocrystalline chromium prepared by evaporating chromium under conditions in which little oxygen was believed to be present had primarily the *A*-15 structure characteristic of β -W. By introducing oxygen into the vacuum system, they reported that the bcc phase was stabilized.^{18,19} Based on this earlier work it was anticipated that sample *A* would contain a significant amount of material having the *A*-15 structure,²⁴ however, this was not the case.

Secondary phases were observed in samples *B* (the air-exposed chromium powder) and *C* (the compacted pellet formed from air-exposed chromium powder). For both samples the primary phase present was bcc chromium (92 wt. %), while secondary *crystalline* phases consisted of *A*-15 chromium (4 wt. %), Cr_2O_3 (2 wt. %), and CrO_3 (2 wt. %). In addition to these phases, the large amount of diffuse scattering—much like that observed in our earlier measurements of sample *E*,⁸ suggests the presence of amorphous phases and/or hydrogen in samples *B* and *C*.

Satisfactory Rietveld refinements (reduced χ^2 values

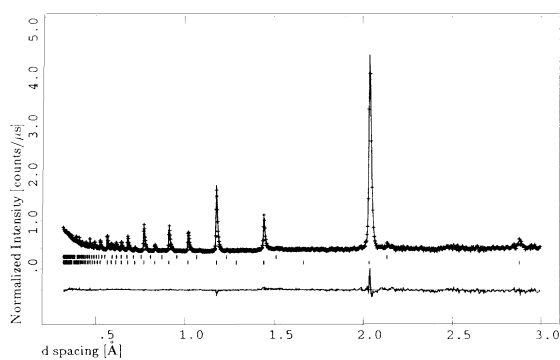


FIG. 1. One of six diffraction patterns taken from sample *A* at 20 K. The data have been normalized to the incident neutron spectrum. The solid line through the data points, +’s, represents the fit to the data obtained from the Rietveld refinement. A curve showing the difference between the data and the fit is found at the bottom of the figure. Positions of Bragg reflections are marked by |’s. The upper row of reflection markers corresponds to reflections from the bcc vanadium lattice of the sample container, while the lower row corresponds to reflections from the bcc chromium lattice.

varied between 2 and 6) were obtained for data from samples *A* and *D* using a single body-centered-tetragonal phase. The tetragonal $I4/mmm$ space group was chosen rather than the cubic space group $Im\bar{3}m$ for chromium so that a magnetic moment could be refined for the commensurate, AF_0 , magnetic structure. The reduced symmetry of the $I4/mmm$ space group is needed, since the magnetic moments of the chromium atoms do not possess threefold rotational symmetry about $\langle 111 \rangle$ directions. While the choice of the $I4/mmm$ space group allowed for the refinement of the AF_0 magnetic structure, this choice did not produce significant changes in refinements of the lattice parameter, particle size, microstrain broadening, or Debye-Waller parameters compared to those obtained when a bcc lattice was chosen and the magnetic Bragg reflection ignored. The insensitivity of these parameters to the presence (or lack) of a magnetic reflection is due to the fact that the magnetic 100 reflection is only one of more than forty reflections with different d -spacings identified in the diffraction patterns.

Data for the magnetic 100 reflection of the four samples at 20 K are shown in Fig. 2. This reflection is forbidden in the bcc structure, but is allowed in a neutron-diffraction experiment for particular ordering of magnetic moments. In the case of chromium, its antiferromagnetically ordered structure has a periodicity along the $[100]$ direction twice that of the nuclear lattice, and so intensity is seen at the 100 reflection when indexed relative to the nuclear lattice. Magnetic 100 reflections were observed from samples *A*, *C*, and *D* at 20 K, indicating that these three samples were antiferromagnetic at this temperature. In contrast, little, if any, intensity above background is seen in the data taken from sample *B*. This observation is particularly significant in light of the fact that when the material used to make sample *B* is compacted to make sample *C* a magnetic 100 Bragg reflection

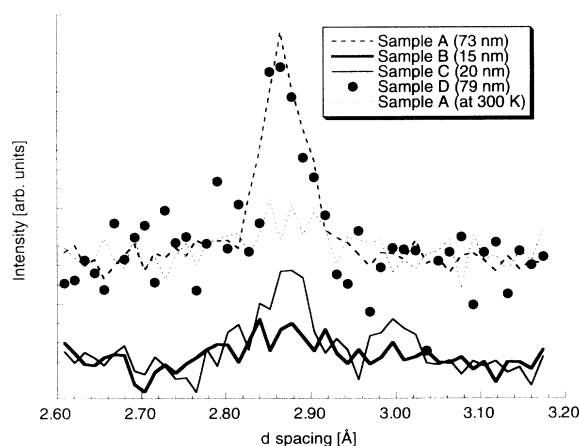


FIG. 2. Portions of the diffraction patterns in the region of the 100 bcc chromium reflection taken from the four samples (*A* through *D* corresponding to dashed, thick solid lines, thin solid lines, and ●’s, respectively) at 20 K with background subtracted. Also shown are the data for sample *A* taken at 300 K (dotted line). The curves were normalized to the products of exposure times and sample masses. The data for samples *B* and *C* have displaced from those of *A* and *D* for the sake of clarity.

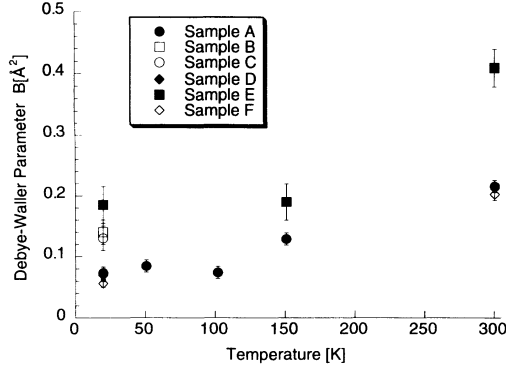


FIG. 3. The Debye-Waller parameters, B , of the different samples plotted versus temperature.

is clearly observed (see Fig. 2). The magnetic 100 reflection was not observed in sample *A* at room temperature (dotted line in Fig. 2) and was very weak at 150 K (a magnetic reflection was only observed in the low-resolution detector banks, while below 150 K the reflection was observed in all the detector banks, including the highest-resolution banks), indicating that antiferromagnetism in sample *A* was suppressed significantly below the Néel temperature of single-crystal or coarse-grained chromium. Data from the other samples at temperatures above 20 K were not obtained, and thus it is not known if the Néel temperature was also suppressed in samples *C* and *D*.

Refinements of the width of the microstrain broadening distribution, ϵ_σ , obtained from the widths of all the Bragg reflections, Debye-Waller parameter, $B = 8\pi^2 \langle u^2 \rangle$, magnetic moment, μ , and particle size, P , for each sample are tabulated in Table I along with results from our previous study⁸ (corrected for absorption) of a compacted nanocrystalline sample and a coarse-grained control sample. An indication as to whether or not antiferromagnetic order was observed in a sample at 20 K is listed in the last column. The data taken from sample *B* are of sufficiently good quality that not more than 23% of the sample could have been antiferromagnetically ordered with a magnetic moment equal to the average of the three other nanocrystalline samples (*A*, *C*, and *D*), otherwise the magnetic 100 Bragg reflection would have been observed. The temperature dependencies of the Debye-Waller parameter for the different samples and the mag-

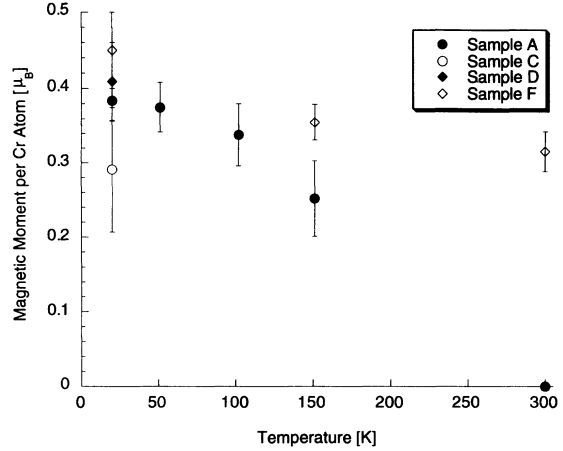


FIG. 4. Magnetic moment per chromium atom in the bcc phase deduced for the 73-nm grain size powder sample (●, sample *A*), 20-nm compacted nanocrystalline sample (◆, sample *D*), 79-nm powder sample (○, sample *C*), and the coarse-grained control sample (◇, sample *F*).

netic moment attributed to the chromium atoms in sample *A* from the Rietveld refinements are shown in Figs. 3 and 4, respectively.

The particle size of sample *B* determined using the Rietveld refinement technique was in excellent agreement with dark-field transmission electron microscopy observations. In our earlier study,⁸ we reported that the particle sizes determined from the diffraction and dark-field microscopy techniques for sample *E* were also in excellent agreement. The consistency between the particle sizes measured with the two techniques gives added confidence that Rietveld refinement of neutron-diffraction data accurately determines the particle sizes of the samples examined in this study.

IV. DISCUSSION

A. Correlations between microstructure and antiferromagnetic ordering

The absence of antiferromagnetism in sample *A* at room temperature is different from the behavior exhibited by the coarse-grained sample (sample *F*), where antiferromagnetic order was observed at and below 323 K. This difference might be attributed to differences in the microstructures of the two samples. There are two major

TABLE I. Parameters from the Rietveld refinements. The asterisk denotes that the bcc phase of sample *E* was not antiferromagnetically ordered; however, the *A*-15 chromium phase of sample *E* was ordered at 20 K, and a moment of $(2.5 \pm 0.2)\mu_B$ calculated for this phase.

Sample	ϵ_σ (%)	B at 20 K (Å ²)	μ (μ _B)	P (nm)	AF at 20 K
<i>A</i>	0.1 ± 0.1	0.07 ± 0.01	0.38 ± 0.05	73 ± 4	yes
<i>B</i>	0.3 ± 0.1	0.14 ± 0.02	0	15 ± 1	no
<i>C</i>	0.3 ± 0.1	0.13 ± 0.02	0.29 ± 0.08	20 ± 2	yes
<i>D</i>	0.1 ± 0.1	0.07 ± 0.01	0.41 ± 0.05	79 ± 5	yes
<i>E</i>	1.0 ± 0.1	0.185 ± 0.025	0*	11 ± 1	no
<i>F</i>	0.7 ± 0.1	0.056 ± 0.008	0.45 ± 0.05		yes

differences. The first is the large amount of long-range microstrain in sample *F*, which produced broadening of the Bragg reflections.²⁵ Microstrain broadening can be separated from particle size broadening, because of their differing dependence on *d* spacing, and the range of *d*-spacings sampled in these experiments is more than adequate to separate these broadening effects. Defects like dislocations and planar interfaces produce microstrain broadening of Bragg reflections.²⁵ Very little, if any, microstrain broadening was observed in the Bragg reflections from sample *A*. Bacon and Cowlam⁹ have shown that the Néel temperature of coarse-grained materials can be increased from the value for strain-free chromium (311 K) to 450 K after heavily deforming the material—a process that usually introduces dislocations. The relative lack of long-range microstrain in sample *A* is not likely to result in the suppression of its Néel temperature. The second major difference between the two samples is their grain sizes. Compared to the coarse-grained sample, sample *A* has a much smaller grain size and a correspondingly larger content of free surfaces.

Differences between the microstructures and/or impurity contents of these samples provide an indication of the cause for the suppression of antiferromagnetism in the bcc portion of sample *B* to temperatures below 20 K. Of the samples listed in Table I, only sample *E* has a smaller grain size than sample *B* (11 nm compared to 15 nm), and the bcc phase of sample *E* also does not exhibit antiferromagnetic ordering at 20 K. Since the two samples with the smallest grain sizes, *B* and *E*, also have the largest area of interfaces, the content of interfaces can be correlated to the suppression of antiferromagnetism. The character of these interfaces appears to be unimportant, since sample *B* contains free surfaces, while sample *E* contains grain boundaries. Samples *B* and *E* were both exposed to air prior to obtaining neutron-diffraction data and thus these samples contain light-element impurity phases. In contrast, sample *C*, which was also exposed to air prior to measurement and so contains some light-element impurity concentrations, is antiferromagnetically ordered at 20 K. This observation suggests that the suppression of antiferromagnetism in nanocrystalline bcc chromium is not solely due to impurities, since if this were the case, sample *C* would not have been antiferromagnetically ordered. Sample *C* has, however, a larger grain size than either sample *B* or *E*. As in the comparison of samples *A* and *F* at 150 K, a correlation between the suppression of antiferromagnetism and small grain size (and correspondingly large content of interfaces) is observed in samples cooled to 20 K.

Interestingly, the two samples in which antiferromagnetism is suppressed at 20 K are also the samples with the largest Debye-Waller parameters. Debye-Waller attenuation of Bragg reflections is caused by thermal motion of atoms and/or static displacements of atoms from their lattice sites due to defects, e.g., vacancies, interstitials, and dislocation loops, with short-range strain fields.²⁵ From measurements of the temperature dependence of the Debye-Waller parameter of sample *E*, we previously showed that the origin of its large value was due to static displacements and not thermal motion.⁸ In

light of this observation and the fact that little thermal motion is expected at 20 K, the enhancements of the Debye-Waller parameters for samples *B* and *C* with respect to the literature²⁶ value of 0.11 \AA^2 are probably due to static displacements arising from defects with short-range fields. These defects may contribute to the suppression of antiferromagnetism at 20 K, but are not primarily responsible for its suppression. If this were the case, antiferromagnetism would not have been suppressed to below 150 K in sample *A*, since the Debye-Waller parameter measured for this sample was not very different from that of sample *F*. Sample *F* was antiferromagnetic above 150 K.

B. Comparisons with other work

In addition to the data taken in the present study, the studies of nanocrystalline chromium powder performed by Tsunoda, Nakano, and Matsuo¹⁶ and Furubayashi and Nakatani¹⁷ can be used to check for consistency with the hypothesis that small grain sizes lead to a suppression of antiferromagnetic order in bcc chromium. The magnetization measurements of Furubayashi and Nakatani¹⁷ on 2-nm grain-sized chromium powder were interpreted as indicating that their powders were paramagnetic over the entire temperature range 4.2–298 K. Our data are consistent with this observation. In contrast, Tsunoda, Nakano, and Matsuo¹⁶ observed antiferromagnetic order of the bcc phase even at room temperature in chromium powder estimated to have an average grain size of 13 nm. Our data indicate that samples with grain sizes less than 16 nm are not antiferromagnetic even at 20 K.

One explanation for this discrepancy between the results of Tsunoda, Nakano, and Matsuo and the present study is that additional unidentified microstructural features could play a role in determining the Néel temperature of nanocrystalline chromium, and that differences in sample preparation procedures existed in the two studies which were important enough to produce such changes. Both studies prepared samples by the gas-condensation process, although Tsunoda, Nakano, and Matsuo¹⁶ used approximately twice the gas pressure compared to the present study. They also used argon rather than helium, which was used in the present study. If similar evaporation rates were used, then the conditions employed by Tsunoda, Nakano, and Matsuo should result in larger grain-sized material than those used in the present work;²⁸ however, no other significant microstructural differences are expected.

Tsunoda, Nakano, and Matsuo¹⁶ annealed their material at 833 K for 5.25 h in order to transform the *A*-15 chromium phase,^{18,19} assumed by them to be the majority phase after evaporation, into the bcc phase. The samples studied here were not annealed. If defects with short-range displacement fields of the type that cause Debye-Waller attenuation could be removed from a nanocrystalline sample without a concomitant increase in grain size, and these defects are a factor in the suppression of antiferromagnetism at 20 K, then magnetic order might be found in samples after annealing when no order was observed prior to annealing.

Another explanation for the disagreement between the two studies is that either the Rietveld refinement procedure overestimated the grain sizes of samples *B* and *E*, or Tsunoda, Nakano, and Matsuo¹⁶ underestimated the grain size of their sample. The former is unlikely to have occurred, since the Rietveld refinement of the particle size is in excellent agreement with the dark-field transmission electron microscopy observations.

The 13-nm grain size reported by Tsunoda, Nakano, and Matsuo is inconsistent with their neutron-diffraction measurements. The full width at half maximum of the 110 reflection is measured to be $\Gamma = 0.026 \text{ \AA}^{-1}$ from Fig. 2 of Ref. 16. Assuming that the breadth of this reflection is determined solely by particle size effects, which ignores the non-negligible contributions from microstrain and instrumental broadening, then the minimum particle size consistent with their neutron observations is no smaller than $2\pi/\Gamma = 24 \text{ nm}$. A possible source of error in the work of Tsunoda, Nakano, and Matsuo comes from the fact that the 13-nm average grain size of their material was determined from x-ray data, and it is implied that the x-ray data were taken from a different sample than that used in their neutron study. It is also not known from Ref. 16 whether the x-ray sample was protected against air exposure. If exposed to air, the crystalline bcc component of a small particle might indeed be smaller than the size of the particle prior to air exposure (the neutron measurements of Tsunoda, Nakano, and Matsuo were taken from a sample that was protected against exposure to air), since the bcc chromium phase would be consumed by oxygen to form a crystalline or amorphous oxide shell about the particle. Regardless of the actual values for the grain sizes of the samples in the present work and that of Tsunoda, Nakano, and Matsuo the grain size of the latter is believed to be significantly greater than that of samples *B* or *E*, and therefore antiferromagnetism is not expected to be suppressed in their sample, nor is it.

The 13-nm average grain size reported by Tsunoda, Nakano, and Matsuo¹⁶ is also inconsistent with an estimate of the grain size of their sample obtained by overlaying their data with intensity profiles for the 110 reflection from our samples *A* and *B* (Fig. 5), whose Rietveld refinements indicate particle sizes of 73 and 15 nm, respectively. Since the breadth of the reflection from sample *B* is larger than that reported by Tsunoda, Nakano, and Matsuo,¹⁶ and if the microstrain and instrumental broadening of the two measurements are comparable (an indication of the instrumental broadening of the HIPD is given by the solid line in Fig. 5), then the average grain size of the Tsunoda, Nakano, and Matsuo sample is significantly larger than 15 nm.

The magnetic moments ranging from (0.29 ± 0.08) to $(0.40 \pm 0.05)\mu_B$ for samples *A*, *C*, and *D* at 20 K are only somewhat smaller than the value obtained for the coarse-grained sample (sample *F*) of $(0.45 \pm 0.05)\mu_B$.²⁹ Bacon and Cowlam⁹ report the peak magnetic moment in antiferromagnetic chromium that is modulated by a spin density wave, i.e., the AF_1 and AF_2 phases, to be $0.59\mu_B$. This corresponds to a root-mean-square (rms) value of $0.42\mu_B$. Since the Rietveld procedure refines a magnetic moment for a commensurate magnetic struc-

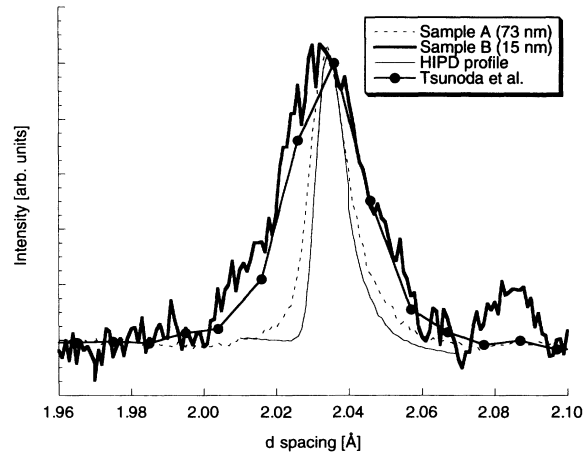


FIG. 5. Profiles of the 110 Bragg reflections from samples *A* and *B*, and that of Tsunoda. The instrumental broadening profile for the high intensity powder diffractometer corresponding to the data of the present investigation is given by the thin solid line. Background intensity was removed from all the profiles.

ture, the rms value of Bacon and Cowlam should be compared to the moments reported for samples *A*, *C*, *D*, and *F*. The agreement is very good. The agreement is also very good with the magnetic moment reported for the AF_0 structure by Bacon and Cowlam⁹ of $0.42\mu_B$.

While the magnetic moment of $(0.29 \pm 0.08)\mu_B$ deduced for sample *C* is not statistically different from those deduced for samples *A* and *D*, the smaller value for sample *C* may be an indication that the entire sample was not antiferromagnetically ordered. For example, if a portion of sample *C* contains grains that were too small to be antiferromagnetically ordered, these grains would not contribute intensity to the magnetic reflection but would contribute intensity to the nuclear Bragg reflections. Thus, if the entire sample were assumed to contribute the magnetic reflection, as was the case for the Rietveld refinement procedure used, then the moment refined for the sample must be correspondingly smaller to account for the relative lack of intensity in the magnetic reflection that would have been present had the entire sample been antiferromagnetically ordered. Since distributions of grain sizes, whose means correspond to particle sizes deduced from Rietveld refinement, are known to be present in samples *B* and *E* from transmission electron microscopy, and sample *C* was compacted from the material used to make sample *B*, sample *C* is also likely to contain a distribution of grain sizes. A portion of sample *C* may be comprised of particles smaller than the mean particle size of 20 nm reported for this sample and may be too small to be antiferromagnetically ordered. Conversely, portions of samples *B* and *E* may be large enough to be antiferromagnetically ordered, consequently these portions may be responsible for intensity, if any, just above background in the region of the 100 Bragg reflection.

Bacon and Cowlam⁹ reported that variations in residual stresses throughout a sample will stabilize the AF_1 and

AF_2 spin-density-wave magnetic structures simultaneously in polycrystalline chromium with average grain sizes of 0.1–2 mm below 300 K. In materials with grain sizes less than 0.1 mm, the two phases were stabilized below 200 K. Above these temperatures and below 450 K, heavily deformed coarse-grained chromium was reported to exhibit the simple nonspin-density-wave commensurate AF_0 structure.⁹ From their observed correlation of grain size and the transition temperature to the spin-density-wave phases, one might conclude that nanocrystalline chromium samples could exhibit the AF_0 structure even at temperatures as low as 20 K. In other words, the magnetic phase diagram of nanocrystalline chromium might be the same as heavily deformed coarse-grained chromium but with transition temperatures scaled down to very low temperatures according to the grain size of the material.

The present data cannot rule out the AF_2 phase in samples *A*, *C*, and *D* at 20 K, since this phase cannot be distinguished from the AF_0 phase. However, if Bacon and Cowlam⁹ are correct that the AF_1 and AF_2 phases are both present in significant quantities at all temperatures where either is present in polycrystalline samples, then the absence of satellite reflections from samples *A*, *C*, and *D* suggests that these samples have the magnetic structure of the AF_0 (commensurate) phase.

C. Possible causes for the suppression of antiferromagnetism in chromium

The trend evident in this work suggests that as the grain size of chromium becomes smaller, the more suppressed the Néel temperature becomes. This trend may be caused by the confinement of the spin density wave in small particles. The spin-density-wave structures in chromium are reported to have a wavelength of about 6 nm.¹² Reducing grain size to similar magnitudes might interfere with the propagation of a spin-density wave and explain the possible absence of antiferromagnetism in nanocrystalline chromium, if the antiferromagnetic structure of ultrafine-grained chromium is modulated by a spin-density wave. A similar difficulty might occur at significantly larger grain sizes, particularly if strain from grain boundaries or surfaces disturb the interiors of chromium grains. The influence of interfacial strain on the properties of nanocrystallites increases with decreasing grain size, since a larger fraction of atoms are disturbed.

Alternatively, the magnetic domain size, i.e., the size of the region in which magnetic order is correlated, in chromium may be an important factor. The smallest domain size reported for the AF_2 phase from measurements of a single-crystal chromium sample cooled through the Néel temperature in the absence of any strong magnetic field is approximately 68 nm.¹² If this value represents the smallest domain size possible, and nanocrystalline chromium exhibits the magnetic structure of the AF_2 phase below the Néel temperature, then only grains with sizes larger than 68 nm would become antiferromagnetically ordered. Sample *C* is antiferromagnetically ordered at 20 K and has a grain size (20

nm) considerably less than 68 nm. This observation suggests that either the smallest domain size possible is less than 20 nm, the domain size is irrelevant, or the antiferromagnetic structure of sample *C* is AF_0 and not AF_2 .

In his overview of surface, interface and thin-film magnetism, Falicov³⁰ states that defects, such as misfit dislocations and stacking faults, can alter the magnetic properties of materials. Indeed, Chrzan *et al.*³¹ have predicted a 2% reduction in the magnetic moment of nickel atoms at {111} stacking faults. They attribute the reduced moment to changes in the environment of nickel atoms at these stacking faults, which broaden the density of states of nickel making the material less magnetic. Owing to the small grain sizes of nanocrystalline materials, a large fraction of atoms reside at or near interfaces (primarily grain boundaries in consolidated samples and free surfaces in unconsolidated powders). Approximately 50% of the atoms in 5-nm grain-sized material are within 0.5 nm of one or more grain boundaries. The atomic relaxations present at or near grain boundaries and surfaces can be correlated to increases in the strain content of nanocrystalline materials. In particular, increases of both long- and short-range strains compared to coarse-grained samples were observed in earlier studies of nanocrystalline palladium^{32,33} and chromium.⁸ In the present study, the samples with the smallest grain sizes contain the most short-range strain. These increases of strain may be partly responsible for the suppression of antiferromagnetic order in nanocrystalline bcc chromium by affecting its density of states like that predicted to occur in nickel. As the grain size of the material is reduced to the nanometer scale, the content of defects producing long- and short-range strain may become so large that they ultimately determine the magnetic properties of the material as a whole. In the case of chromium, the reduction of grain size ultimately leads to the suppression of antiferromagnetic order. This observation has very important technological implications, since, for example, a loss of magnetic order (antiferromagnetic or ferromagnetic order) in nanometer-grain-sized recording media would be undesirable.

Some calculations^{34,35} have predicted, and at least one experiment³⁶ has observed ferromagnetic ordering at the surface of a planar chromium film. If the surfaces of nanocrystalline chromium particles, or perhaps the grain boundaries between these particles, were ferromagnetic rather than antiferromagnetic, a lessening of the intensity of the magnetic 100 reflection is expected. This effect would be observed as a reduction in the magnetic moment calculated by the Rietveld refinement, due to the fact that the refinement assumes the bcc chromium phase to be entirely antiferromagnetic. Indeed, a correlation was observed between magnetic moment magnitude and grain size (see Table I). In order to account for the reduction of the magnetic moment from $0.45\mu_B$ for the coarse-grained sample to $0.29\mu_B$ measured for sample *C*, and assuming the magnetic moments of chromium atoms in the antiferromagnetic phase should have been no different than those in coarse-grained chromium, about 40% of sample *C* would be antiferromagnetic. The remaining outer 2 nm of the particles in sample *C* would

be ferromagnetic. If the outer 2 nm of the particles in sample *E* were also ferromagnetic, then about 25% of this sample would be antiferromagnetic. A reduction of the magnetic 100 reflection observed in sample *C* by one fourth would probably not have been detected, nor is a reflection observed in the diffraction pattern of sample *E*. In other words, parts of sample *E* might be antiferromagnetic at 20 K, but are confined to such small regions that their contribution to the magnetic 100 reflection would be so small (or broad) as not to be measurable.

In our earlier study,⁸ the magnetization of the saturated (ferromagnetic) component of a portion of sample *E* was found using superconducting quantum interference device magnetometry to be 0.0018 emu. If 75% of sample *E* were composed of ferromagnetic shells surrounding antiferromagnetic cores, and the density of a shell is assumed to be the same as bulk chromium, then the saturation magnetization of the shells is calculated to be no more than 2 emu/cm³. Using the moment of $2.2\mu_B$ predicted by Hasegawa³⁴ for a chromium atom on a surface, a saturation magnetization nearly 1000 times larger would have been anticipated. While the correlation between decreasing grain size and an apparent suppression of antiferromagnetism might be explained in terms of antiferromagnetic particles surrounded by 2-nm-thick ferromagnetic shells, the disparity between the saturation magnetization of a shell and that calculated for a chromium surface is so large as to make the explanation implausible.

V. CONCLUSIONS

The effects of grain size, consolidation, and air exposure on the presence of antiferromagnetic order in nano-

crystalline chromium were examined by neutron powder diffraction. In combination with observations from an earlier study, two instances were observed where antiferromagnetism on bcc chromium with the structure of the bulk was suppressed to temperatures below 20 K. Both instances occurred in the samples with the smallest grain sizes (and correspondingly the largest interfacial content). These samples also had large Debye-Waller parameters in comparison with the coarse-grained sample; an observation which suggests that short-range strain may play a role in the suppression of antiferromagnetic order. The presence of short-range strain is not a sufficient condition for the suppression of antiferromagnetism, since antiferromagnetic order was also not observed at room temperature in a third sample, sample *A*, which contained very little, if any, short-range strain. No other characteristic, including amount of microstrain broadening, type (surface or grain boundary) of interfacial content, or the presence of light-element impurities, could be correlated to the suppression of antiferromagnetism in bcc chromium at any temperature. These features have at most a secondary effect on the suppression of antiferromagnetism.

ACKNOWLEDGMENTS

This work was supported by the U.S. Department of Energy, BES-DMS, under Contract Nos. W-31-109-Eng-38 and W-7405-Eng-36. We are grateful to Dr. A. C. Lawson and Dr. R. A. Robinson for valuable discussions. The Manuel Lujan Jr., Neutron Scattering Center is a national user facility funded by the U.S. Department of Energy, Office of Basic Energy Science.

-
- ¹W. Wagner, A. Wiedenmann, W. Petry, A. Geibel, and H. Gleiter, *J. Mater. Res.* **6**, 2305 (1991).
- ²A. Krämer, J. Jing, and U. Gonser, *Hyperfine Interact.* **54**, 591 (1990).
- ³J. C. Mallinson, in *Magnetic Properties of Materials*, edited by J. Smit (McGraw-Hill, New York, 1971), pp. 245–257.
- ⁴U. Herr, J. Jing, R. Birringer, U. Gonser, and H. Gleiter, *Appl. Phys. Lett.* **50**, 472 (1987).
- ⁵H.-E. Schaefer, H. Kisker, H. Kronmüller, and R. Würschum, *NanoStr. Mater.* **1**, 523 (1992).
- ⁶R. Birringer, U. Herr, and H. Gleiter, *Suppl. Trans. Jpn. Inst. Met.* **27**, 43 (1986).
- ⁷L. Daróczy, D. L. Beke, G. Posgay, G. F. Zhou, and H. Bakker, *NanoStr. Mater.* **2**, 515 (1993).
- ⁸M. R. Fitzsimmons, J. A. Eastman, R. A. Robinson, A. C. Lawson, J. D. Thompson, R. Movshovich, and J. Satti, *Phys. Rev. B* **48**, 8245 (1993).
- ⁹G. E. Bacon and N. Cowlam, *J. Phys. C* **2**, 238 (1969), Ser. 2.
- ¹⁰W. C. Koehler, R. Moon, A. L. Trego, and A. R. MacKintosh, *Phys. Rev.* **151**, 405 (1966).
- ¹¹E. Fawcett, *Rev. Mod. Phys.* **60**, 209 (1988).
- ¹²E. Fawcett, R. Griessen, and D. J. Stanley, *J. Low Temp. Phys.* **25**, 771 (1976).
- ¹³M. O. Steinitz, D. A. H. Pink, and D. A. Tindall, *Phys. Rev. B* **15**, 4341 (1977).
- ¹⁴G. Herzer, *IEEE Trans. Mag.* **26**, 1397 (1990).
- ¹⁵G. Herzer, *Mater. Sci. Eng. A* **133**, 1 (1991).
- ¹⁶Y. Tsunoda, H. Nakano, and S. Matsuo, *J. Phys. Condens. Matter* **5**, L29 (1993).
- ¹⁷J. A. Eastman, L. J. Thompson, and D. J. Marshall, *NanoStr. Mater.* **2**, 377 (1993).
- ¹⁸K. Kimoto and I. Nishida, *J. Phys. Soc. Jpn.* **22**, 744 (1967).
- ¹⁹C. G. Granqvist, G. J. Milanowski, and R. A. Buhrman, *Phys. Lett.* **54A**, 245 (1975).
- ²⁰A. C. Lawson, J. A. Goldstone, J. G. Huber, A. L. Giorgi, J. W. Conant, A. Severing, B. Cort, and R. A. Robinson, *J. Appl. Phys.* **69**, 5112 (1991).
- ²¹A. C. Larson and R. B. Von Dreele (unpublished).
- ²²J. K. Warner, A. K. Cheetham, A. G. Nord, R. B. Von Dreele, and M. Yethiraj, *J. Mater. Chem.* **2**, 191 (1992).
- ²³J. K. Warner, A. K. Cheetham, D. E. Cox, and R. B. Von Dreele, *J. Am. Chem. Soc.* **114**, 6074 (1992).
- ²⁴J. A. Eastman, M. R. Fitzsimmons, K. E. Sickafus, and L. J. Thompson (unpublished).
- ²⁵M. A. Krivoglaz, *Theory of X-Ray and Thermal-Neutron Scattering by Real Crystals* (Plenum, New York, 1969).
- ²⁶*International Tables for X-Ray Crystallography III*, edited by C. H. Macgillavry and G. D. Rieck (Reidel, Dordrecht, 1983).
- ²⁷T. Furubayashi and I. Nakatani, *J. Appl. Phys.* **73**, 6412 (1993).
- ²⁸C. G. Granqvist and R. A. Buhrman, *J. Appl. Phys.* **47**, 2200

(1976).

- ²⁹The value of $(0.37 \pm 0.03)\mu_B$ obtained from the Rietveld refinement of the 20 K data for sample *F* was increased by the square root of the fractional intensity appearing in the satellite reflections, which is not accounted for in the refinement. After accounting for this intensity, a value of $(0.45 \pm 0.05)\mu_B$ was obtained.
- ³⁰L. M. Falicov, *Thin Solid Films* **216**, 169 (1992).
- ³¹D. C. Chrzan, L. M. Falicov, J. M. MacLaren, X.-G. Zhang, and A. Gonis, *Phys. Rev. B* **43**, 9442 (1991).
- ³²M. R. Fitzsimmons, J. A. Eastman, M. Müller-Stach, and G. Wallner, *Phys. Rev. B* **44**, 2452 (1991).
- ³³J. A. Eastman, M. R. Fitzsimmons, and L. F. Thompson, *Philos. Mag. B* **66**, 667 (1992).
- ³⁴H. Hasegawa, *J. Phys. F* **16**, 1555 (1986).
- ³⁵R. H. Victora and L. M. Falicov, *Phys. Rev. B* **31**, 7335 (1985).
- ³⁶L. E. Klebanoff, R. H. Victora, L. M. Falicov, and D. A. Shirley, *Phys. Rev. B* **32**, 1997 (1985).